ELSEVIER

Journal of Nuclear Materials 317 (2003) 234–242

journal of nuclear materials

www.elsevier.com/locate/jnucmat

Application of the local fracture stress model on the cleavage fracture of the reactor pressure vessel steels in the transition temperature region

Won-Jon Yang [a], Bong-Sang Lee [b,*], Moo-Young Huh [a], Jun-Hwa Hong [b]

[a] *Division of Materials Science and Engineering, Korea University, Seoul 136-701, South Korea*
[b] *Nuclear Material Technology Development, Korea Atomic Energy Research Institute, Yuseong P.O. Box 105, Daejeon 305-600, South Korea*

Received 30 May 2002; accepted 18 February 2003

Abstract

The fracture toughness in the ductile–brittle transition region of reactor pressure vessel steels was evaluated by means of an RKR-type model which describes the temperature dependence of the cleavage fracture toughness based on the constant fracture stress σ_f. The fracture stress σ_f and the characteristic distance are two main parameters in the RKR model. In order to apply the RKR model to the transition temperature region, these two parameters were investigated in different manners. In this study, the local fracture stress, σ_f^*, was determined from the pre-cracked specimens. The results showed that the local fracture stress σ_f^* determined from the pre-cracked specimens was higher than the fracture stress σ_f from the notched specimens, while those values were practically independent of the temperatures. The CID (cleavage initiation distance), which represents the distance from the crack tip to the cleavage initiation site, was measured in every fractured specimen. The measured CID values were strongly dependent on the test temperatures. Besides, the fracture toughness K_{JC} in the transition region was dependent on the measured CID. The RKR model, when the local fracture stress σ_f^* and the measured CIDs were applied, could describe the temperature dependency of the median transition fracture toughness $K_{JC(med)}$.

PACS: 81.40.Np; 81.70.Bt; 81.05.Bx; 62.20.Mk

1. Introduction

It is generally accepted in the micromechanistic models of cleavage fracture that the critical events are controlled by the fracture stress [1–10]. The models have explained that the cleavage fracture occurs when the principal stress exceeds the fracture stress σ_f over a certain region in front of crack tip. It is known that the σ_f is independent of temperature, strain rate, etc. The value of σ_f has been determined mainly from rigid plastic solutions for notched specimens loaded in plane strain bending. To evaluate the fracture stress in notched specimen, Hill's method [11] has been used by many researchers, and the results have showed the constancy of σ_f for low temperature cleavage fracture. Griffith and Owen [12] have analyzed data sets for cleavage initiation in iron, with performing the stress analysis of 45° V-notched specimens of macroscopic root radius ($\rho = 0.25$) with an elastic–plastic finite element method. They also found that σ_f was not sensitive in the relatively wide temperature range. Wang and Chen [13] showed that σ_f still remains constant with increasing notch depth and notch flank angle. Bowen et al. [14] found that σ_f appears to be independent of temperature for any given microstrucural condition.

* Corresponding author. Tel.: +82-42 868 8561; fax: +82-42 868 8346.
E-mail address: bongsl@kaeri.re.kr (B.-S. Lee).

0022-3115/03/$ - see front matter © 2003 Published by Elsevier Science B.V.
doi:10.1016/S0022-3115(03)00106-5

Nomenclature

E	elastic modulus	K_{JC}	elastic–plastic fracture toughness derived from J-integral
σ_0	yield strength	$K_{JC(med)}$	median value of K_{JC}
σ_{nom}	nominal bending stress	J_{app}	applied J-integral
$\sigma_{11,max}$	maximum value of σ_{11}	ρ	notch root radius
σ_{yy}	longitudinal tensile stress (maximum principal stress)	X	distance from the crack tip
σ_f	fracture stress	n	work-hardening exponent
σ_f^*	local fracture stress	CID	Cleavage initiation distance which is the distance from crack tip to cleavage triggering point
K_{IC}	plane strain fracture toughness		

Richie, Knott and Rice (RKR) [15] have proposed a cleavage fracture model to predict the temperature dependence of plane strain fracture toughness of pre-cracked specimen using the constant fracture stress with temperature dependency of tensile flow properties. The RKR model says that unstable cleavage fracture occurs when the principal stress σ_{yy} in front of the crack tip exceeds the fracture stress σ_f over a characteristic distance, which was assumed as twice the grain size in the mild steel. The model has been mainly used to evaluate the plane strain fracture toughness K_{IC} related with the cleavage fracture in the lower shelf region.

In the transition region of the structural steels, the fracture toughness increases drastically with increasing temperatures and shows substantial scatter at the same condition [16,17] while fracture still occurs in an unstable cleavage manner.

In this study, an RKR model has been investigated to explain the fracture toughness behaviors of the reactor pressure vessel steels in the transition region where the fracture occurs in the same cleavage manner. Two main parameters which are the fracture stress σ_f and the characteristic distance were defined in different manners. The fracture stress σ_f and the local fracture stress σ_f^* were determined from the notched and the pre-cracked specimens, respectively, based on the stress distribution of each specimen type. The values of CID (cleavage initiation distance), which is defined as the distance from the crack tip to the cleavage initiation site, were measured on all fracture toughness specimens. The fracture toughness of the materials in the transition region was evaluated by the ASTM E 1921-97 [18] standard method which determines the cleavage fracture toughness $K_{JC(med)}$ as a statistical mean value based on the weakest-link theory [19] and Weibull statistics [20] in the transition region.

2. Experimental

The materials used in this study are two different reactor pressure vessel steels, which are an SA 533-B1 plate (JRQ) and an SA 508-3 steel forging (JFL), respectively. The chemical compositions of the test materials were summarized in Table 1.

Test materials were all actual scale forgings or plates thicker than 225 mm. The specimens were sampled only from $1/4T$ location of each block. The orientation of the specimen was the T–L direction. The fracture toughness was evaluated according to the ASTM standard E 1921-97 by using the PCVN specimen (Pre-cracked Charpy V-Notch specimen, $10 \times 10 \times 55$ mm) at various temperatures. In order to determine the fracture stress σ_f, the 4PB notch specimen (four-point bending, $\rho = 0.25$ mm, $12.7 \times 12.7 \times 80$ mm thick) were also tested at −196 and −140 °C. Tensile specimens with 6.2 mm diameter and 25.4 mm gage length were tested over a temperature range of −196 to 25 °C to obtain the yield strength and work-hardening exponent.

All tests were performed in the displacement control with an MTS servo-hydraulic test machine equipped with a high-resolution data acquisition system.

Table 1
The chemical composition of tested materials

Material	Chemical composition (wt%)									
	C	Si	Mn	P	S	Ni	Cr	Mo	Al	Cu
JRQ	0.18	0.24	1.42	0.017	0.004	0.84	0.12	0.51	0.014	0.14
JFL	0.17	0.25	1.44	0.004	0.002	0.75	0.2	0.51	0.116	0.01

Thermocouples were spot-welded on the specimen and test temperatures were controlled within ±1 °C by circulating liquid nitrogen in the isopentane fluid bath. The load-line displacement rate in the fracture toughness test and in the 4PB notch test were 0.5 mm/min and 1 mm/min, respectively. Strain rate in the tensile test was 0.0005/s.

3. Experimental results

3.1. Microstructures

Microstructures of the tested materials were shown in Fig. 1. Both materials showed the typical tempered bainitic microstructures. In order to determine the characteristic distance, the prior austenite grain size was measured by using an image analyzer. The difference of the grain size was not large between two materials, 30 μm (JRQ) and 25 μm (JFL), respectively.

3.2. Tensile and fracture toughness test results

The variation of the yield strength of test materials as a function of temperature was shown in Fig. 2. With decreasing temperature, yield strengths of both steels increase. JRQ has slightly higher yield strength than JFL. The values of the work-hardening exponent were similar in both materials as shown in Fig. 3.

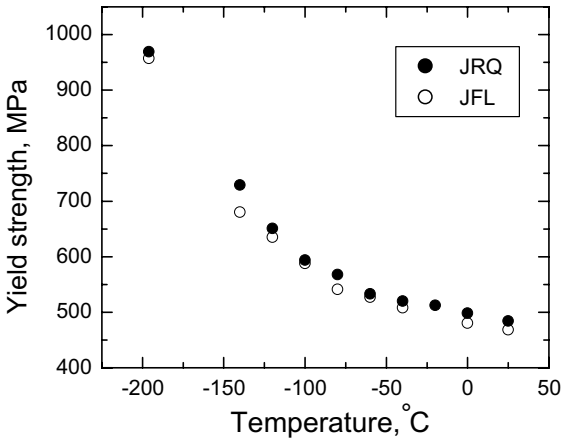

Fig. 2. The variation of the yield strength as a function of temperature.

The fracture toughness values K_{JC} in the transition region were determined for each specimen from J value at the onset of the cleavage fracture, J_c, as follows:

$$K_{JC} = \sqrt{J_C \cdot E}, \tag{1}$$

where E is the elastic modulus. Fig. 4 represents the K_{JC} values determined from equation (1) for JRQ and JFL materials at test temperatures. The behavior of the fracture toughness has a typical form of the structural steels in the transition region. The lines represent the

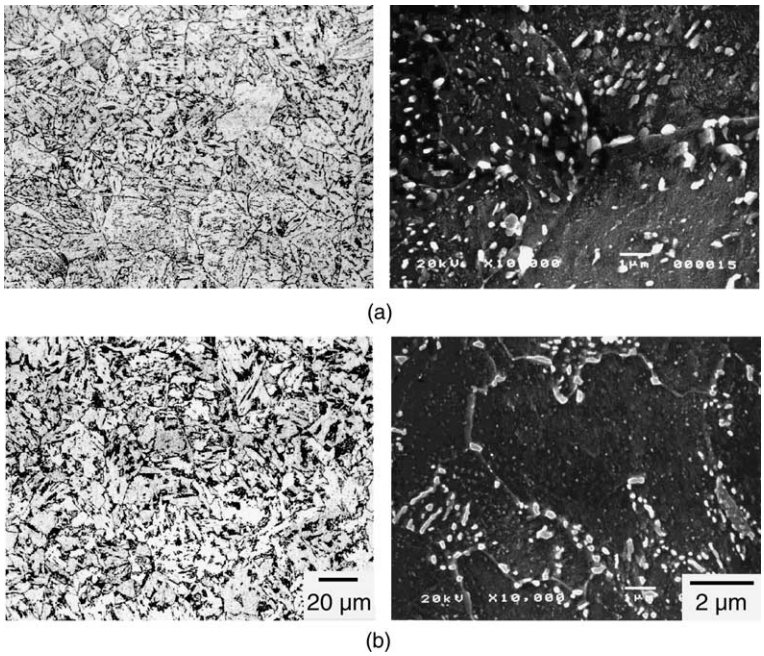

Fig. 1. The microstructures of the tested materials: (a) JRQ and (b) JFL.

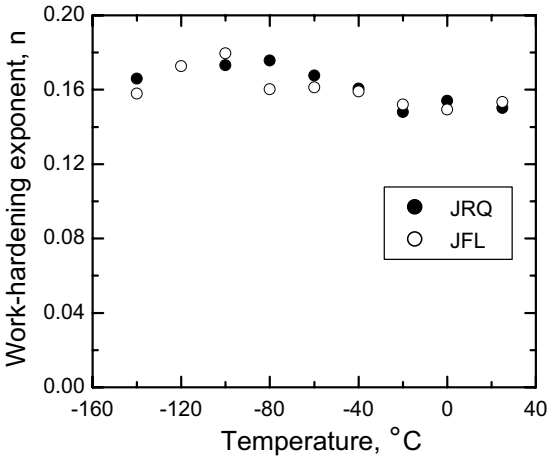

Fig. 3. The variation of the work-hardening exponent as a function of temperature.

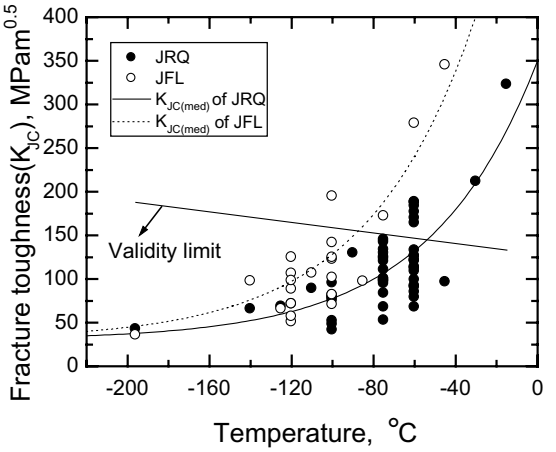

Fig. 4. Transition fracture toughness (K_{JC}) behaviors of the tested materials.

behaviors of the $K_{JC(med)}$ which means a statistical mean value of the fracture toughness. As shown in Fig. 4, JFL material has the higher fracture toughness values than JRQ material in the transition region.

3.3. Determination of the fracture stress σ_f from the conventional notched specimen

To apply the RKR model for the evaluation of the fracture toughness in the transition region, first of all, the fracture stress σ_f of the material should be determined.

An estimate of the fracture stress σ_f for the notched specimen was determined from the slow 4PB test. First, the nominal bending stress, σ_{nom}, the stress at the notch root is found by elasticity theory as follows:

$$\sigma_{nom} = 6M/Bb^2, \tag{2}$$

where M is the applied bending moment, b is the specimen depth below the notch, and B is the specimen thickness. The load on the specimen can be expressed by σ_{nom}/σ_0. By using σ_{nom}/σ_0, the value of fracture stress σ_f in the notched specimen can be calculated from the normalized Griffith–Owen stress intensification plot obtained by numerical calculations in Fig. 5 [12]. It was assumed that the fracture initiates at the position of $\sigma_{11,max}$ ahead of the notch root. This method is generally used to determine the fracture stress of material in other

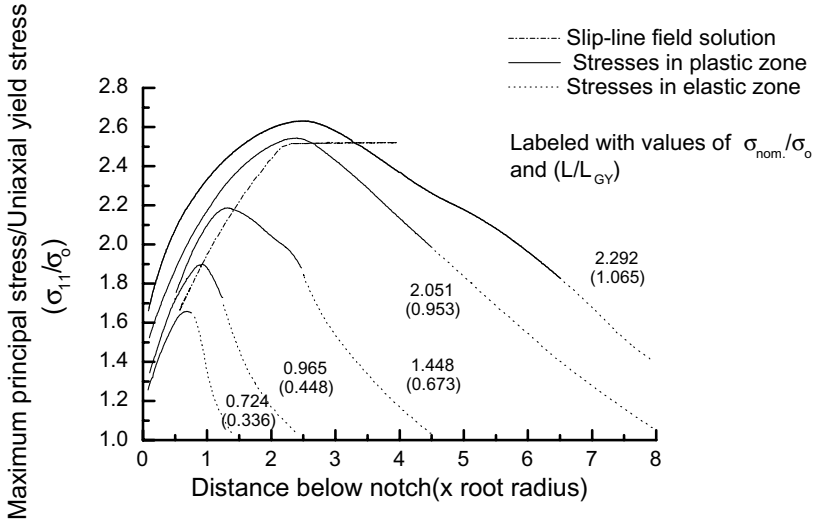

Fig. 5. The variation of the maximum principal stress below the notch at various load conditions, after Griffith and Owen [12].

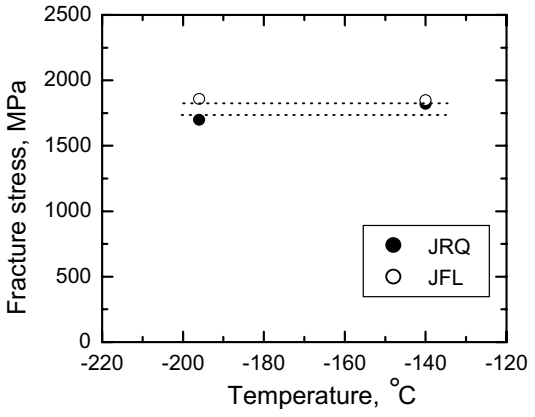

Fig. 6. The behaviors of the fracture stress σ_f from notched specimens as a function of temperature.

Table 2
The fracture stress σ_f of the tested materials in the notched specimen

Material	JRQ		JFL	
Temperature (°C)	−196	−140	−196	−140
Fracture stress σ_f (MPa)	1698	1819	1860	1849
	Ave. 1759		Ave. 1854	

researchers [7,21]. The value of σ_f determined from the notched specimen was summarized in Table 2 and displayed in Fig. 6. Fig. 6 showed JFL material has a slightly higher value than JRQ but σ_f was not sensitive to the test temperature.

3.4. Determination of the local fracture stress σ_f^* from the pre-craked specimen

In this study, σ_f^* was also determined from the pre-cracked specimen to compare with the σ_f. To determine the σ_f^* in the pre-cracked specimen, the value of CID, which was the distance from the crack tip to the cleavage initiation point shown in Fig. 7, was measured in all fractured specimens after testing. The stress field ahead of crack tip by McMeeking [22] was used to determine the local fracture stress in pre-cacked specimen as shown in Fig. 8. The local fracture stress σ_f^* in the pre-cracked specimen, in this study, was defined as the principal stress at CID as shown in Fig. 9. The results of the determined local fracture stress were summarized in Table 3 and shown in Fig. 10. The local fracture stress σ_f^* of JFL was larger than that of JRQ, while their values were also practically independent of temperatures as like results in the notched specimen. Fig. 11 showed that the local fracture stress σ_f^* determined from the pre-cracked

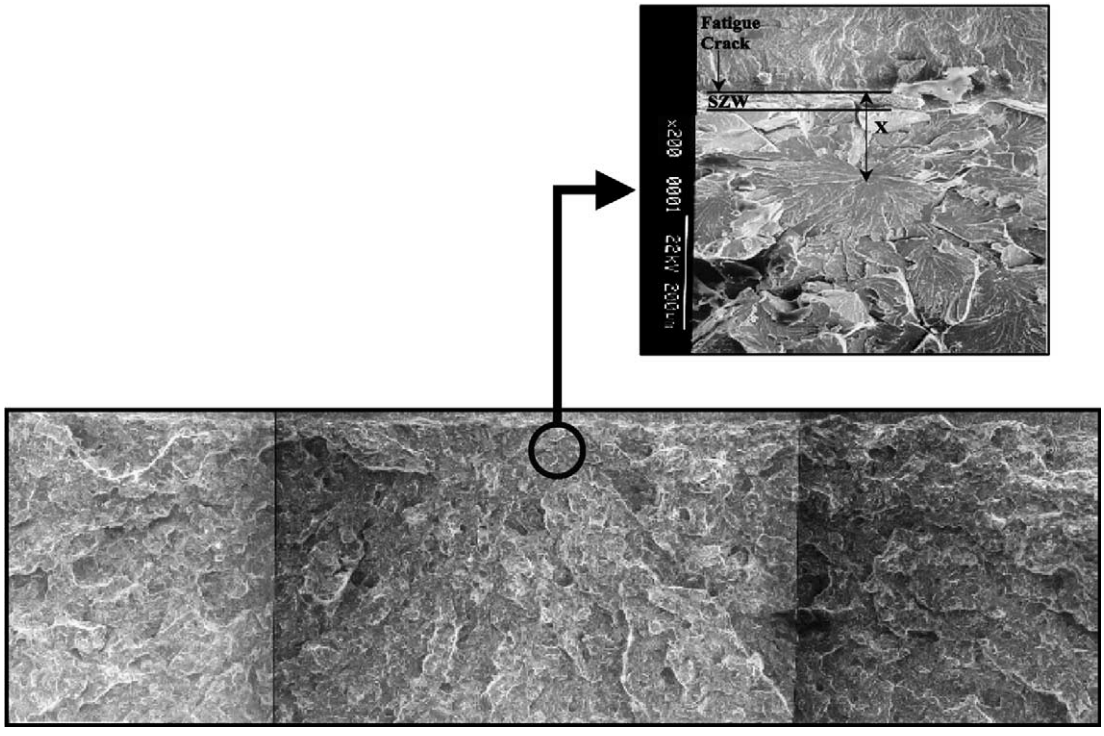

Fig. 7. The measurement of the cleavage initiation distance in the fractured surface.

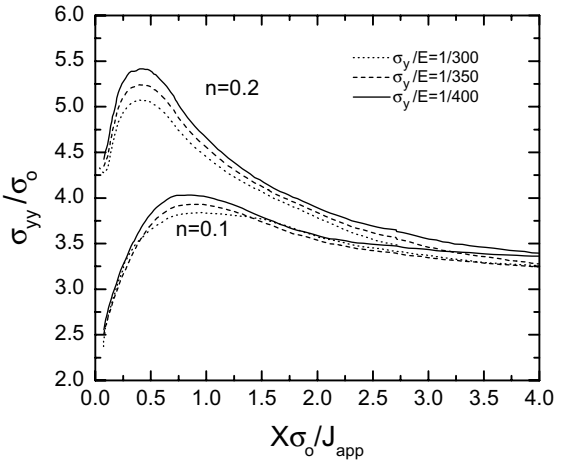

Fig. 8. Stress distribution in front of crack tip by McMeeking's results [22].

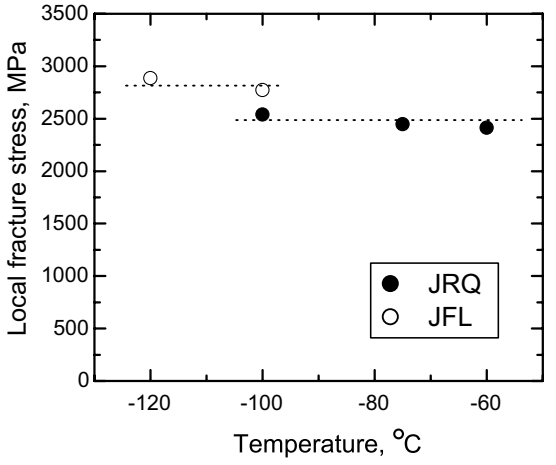

Fig. 10. The behaviors of the local fracture stress σ_f^* from pre-cracked specimens as a function of temperature.

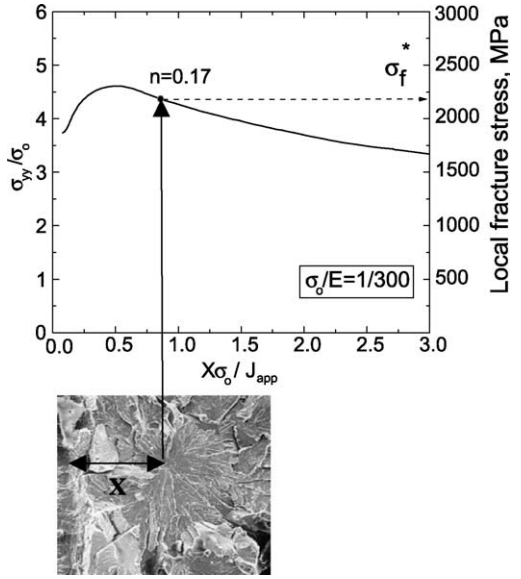

Fig. 9. The determination of the local fracture stress by using the stress field in front of crack tip and measured CID.

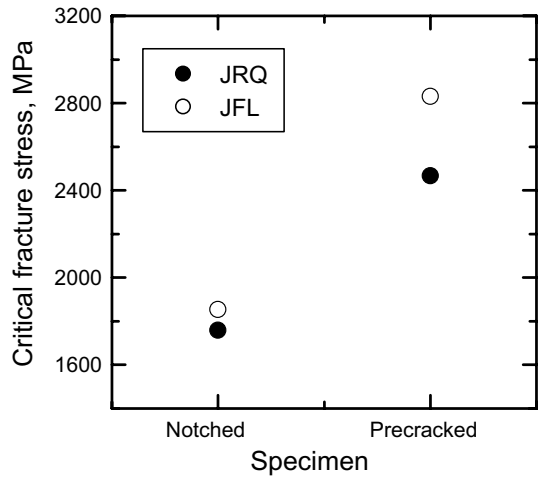

Fig. 11. Comparison of the critical fracture stresses, σ_f^* and σ_f, as specimen types.

Table 3
The local fracture stress σ_f^* of the tested materials in the pre-cracked specimen

Material	JRQ			JFL	
Temperature (°C)	−100	−75	−60	−120	−100
Local fracture stress σ_f^* (MPa)	2538	2447 Ave. 2466	2414	2887 Ave. 2830	2773

specimen was higher than the fracture stress σ_f from the notched specimen.

3.5. Determination of the characteristic distance

Another important variable in RKR model is the characteristic distance which had been assumed as a material parameter. RKR were able to predict the temperature dependence of plane strain fracture toughness by assuming the characteristic distance as two grain size in the mild steel. These values become 60 and 50 μm for JRQ and JFL, respectively, from metallurgical analysis.

4. Discussion

After determining the fracture stress σ_f and the characteristic distance, the fracture toughness of the tested materials as a function of temperature could be predicted from the stress intensification curve shown in Fig. 12 for the given tensile flow properties [23,24]. By taking the fracture stress σ_f and the yield strength σ_0 (Fig. 2) at test temperatures, a measure of plastic zone size (in terms of $(K/\sigma_0))^2$), and hence the fracture toughness could be calculated as the variations of the temperatures. The results of these calculations for both steels were presented in Fig. 13. In Fig. 13, the open circle means the measured value of K_{JC} determined from Eq. (1) and the solid line represent the behaviors of a statistical mean value $K_{JC(med)}$ as the variations of the temperature. The dotted lines are the estimated fracture toughness value when the σ_f and σ_f^* were applied with the characteristic distance defined as two grain size, respectively. As shown in Fig. 13, RKR model was successful for evaluating the lower bound fracture toughness in the lower temperature region in case that σ_f determined from notched specimen was applied. The results of this approach have shown the good agreements with the experimental data of other studies [8,15] for the prediction of the K_{IC}. In addition, in case that σ_f^* determined from the pre-cracked specimen was applied, the predictions seemed to be similar to the median behavior of the $K_{JC(med)}$ in the lower temperature range. However, in the transition region where fracture toughness increases rapidly with increasing temperatures, this model may not characterize the fracture toughness $K_{JC(med)}$ behaviors. This seemed to be related to the reason that the characteristic distance was treated as a constant value in the all temperature range including the transition region. There is, of course, no basic reason for the characteristic dimension to equal precisely two grain size.

The characteristic distance, in RKR model, was defined as a material parameter which was related to the grain size. The predictions of the fracture toughness values shown in Fig. 13 were performed by using the constant characteristic distance. In the lower temperature region, the stress intensification location is very closed to the crack tip and hence cleavage initiation ($\sigma_{yy} > \sigma_f$ at a point) can occur at the distance of the two grain size or less than two grain size. Therefore, the characteristic distance which was a constant in RKR model is sufficient to evaluate the lower bound fracture toughness K_{IC}. With increasing temperature, the necessary stress intensification, however, should be reached at a much larger area in front of the crack tip. As above explanations, because RKR model was originally suggested to predict the plane strain fracture toughness K_{IC}, this model is more adequate in the lower temperature range than in the transition temperature region. In order to apply the RKR model in the transition region, in this study, the CID values, which had been obtained from the fractographical analysis, were regarded as the characteristic distance suggested in the RKR model. De-

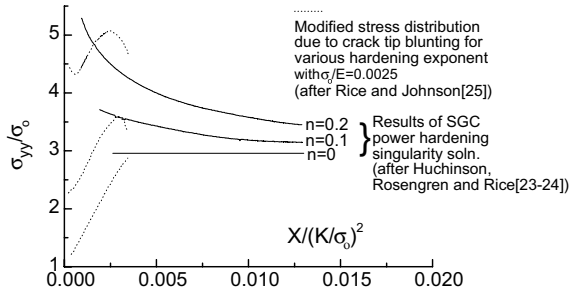

Fig. 12. Stress field in front of crack tip by R&J and HRR, after Rice and Johnson [25].

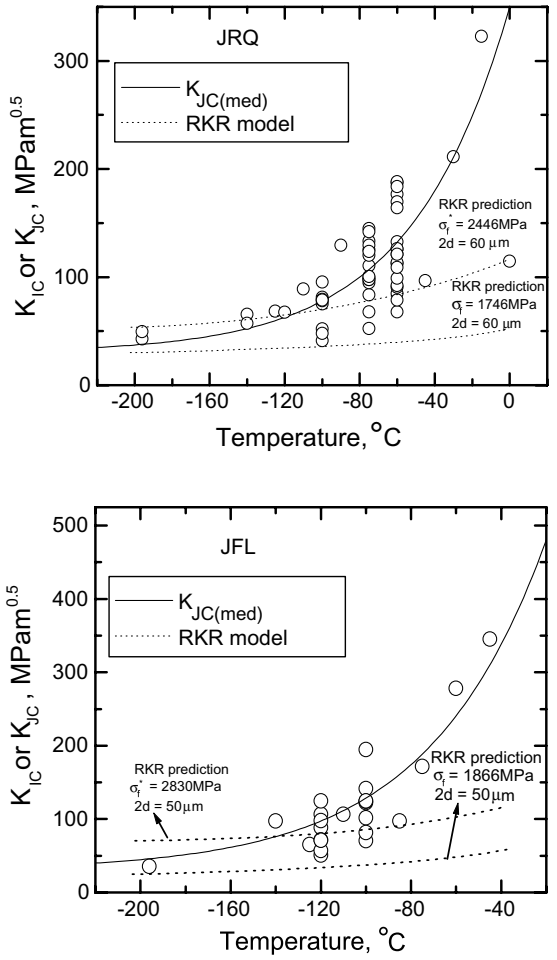

Fig. 13. The behaviors of the predicted fracture toughness by RKR model.

tailed examination on the fractured surfaces was performed to locate the actual cleavage initiation. The measured CID values, in this study, showed no relationship between the two grain size assumed in the RKR model and they were strongly dependent on the temperatures with the statistical distribution as shown in Fig. 14. Cleavage fracture initiates at the nearer location than the distance of the two grain size away from crack tip in the lower temperature region, whereas cleavage fracture occurs at the distance far away two grain size in the higher temperature range. The solid lines in Fig. 14 were drawn by a curve fitting method. Fig. 15 also showed that the fracture toughness K_{JC} was dependent on the CID in the transition region. These results were very closed to Curry and Knott's study [26] which proposed that the characteristic distance is determined by the statistical competition of the carbide particles initiating the cleavage fracture in front of the crack tip. Since the tendency of cleavage fracture decreases when the plastic flow occurs easily as temperature increases, the longer microcrack may be required to induce cleavage fracture at higher transition temperature range. This implies that larger volume of material would be involved

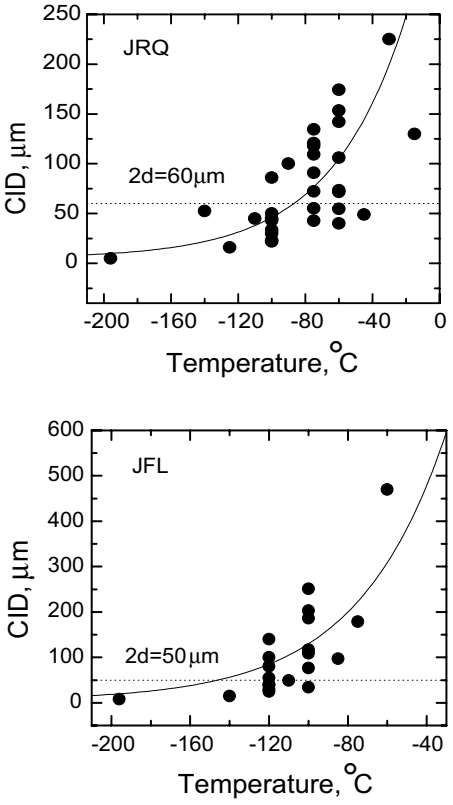

Fig. 14. The variation of the CID values as a function of temperature.

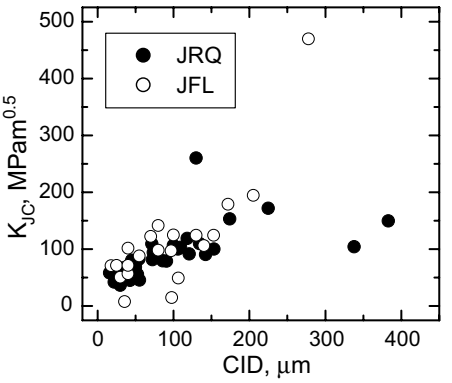

Fig. 15. The relationship between the fracture toughness and the CID values in the transition region.

in the cleavage fracture process to find out larger eligible carbides statistically as increasing temperature. Experimental results showed that the cleavage initiation

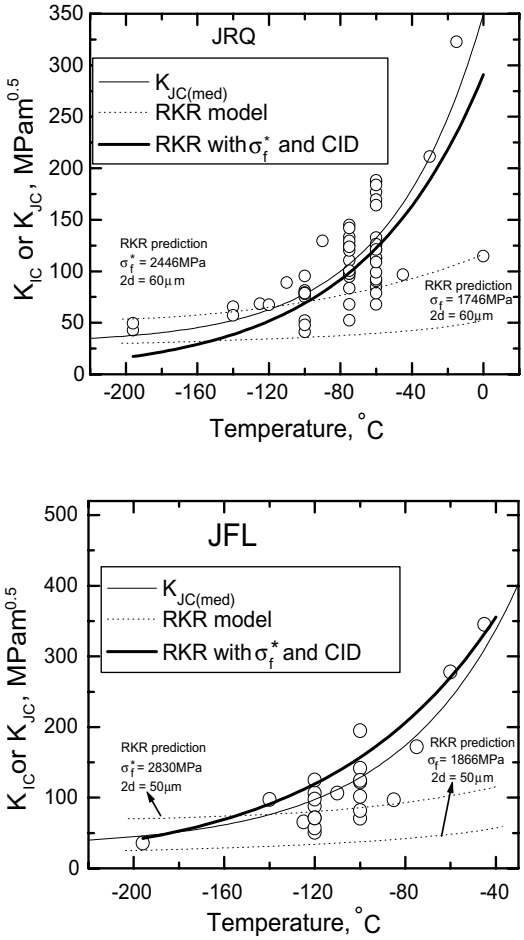

Fig. 16. The behaviors of the predicted fracture toughness by RKR model with σ_f^* and CID.

distance is related to the test temperature in this study. Therefore, the behavior of the CID should be considered for the application of the RKR model to the evaluation of the fracture toughness in the transition region.

Therefore, to apply the RKR model in the transition region where cleavage fracture occurs, in this study, the local fracture stress σ_f^* determined from the pre-cracked specimen and the behaviors of the measured CID which was dependent on the temperatures substituted the two main parameters of the model; the fracture stress σ_f determined from the notch specimen and the characteristic distance assumed as two grain sizes, respectively. In this case, the fracture toughness (J_{app}) could be estimated from Fig. 8 using the known values such as σ_{yy} (σ_f^*), σ_0, and X(CID). The results for this estimation were summarized in Fig. 16. In Fig. 16, the dotted lines were the same one shown in Fig. 13. The thick solid lines represents the estimation results using the σ_f^* and the CID values. The RKR model, when the local fracture stress σ_f^* and the measured CIDs were applied, could describe the temperature dependency of the transition fracture toughness $K_{JC(med)}$ as shown in Fig. 16. It was considered that the CID as well as the local fracture stress σ_f^* may be a main control factor determining the fracture toughness characteristics in case of the applicability of the fracture stress model in the transition temperature region.

5. Conclusions

The applicability of an RKR-type fracture stress model, for describing the cleavage fracture in the transition temperature range of the reactor pressure vessel steels, was investigated. The following conclusions were drawn from the test results:

1. The RKR model, with the values of the fracture stress σ_f determined from the notch specimen and the characteristic distance suggested as the two grain size, was successful for evaluating fracture toughness in the lower temperature region. However, in the transition region where fracture toughness increases drastically with increasing temperatures, this model is not sufficient to characterize the fracture toughness $K_{JC(med)}$ behaviors.
2. The measured CID values, in this study, showed no relationship with the two grain sizes assumed in the RKR model, and they were strongly dependent on the temperatures with the statistical distribution. Besides, the fracture toughness K_{JC} was dependent on the CID in the transition region.
3. The RKR model, when the local fracture stress σ_f^* and the measured CIDs were applied, could describe the temperature dependency of the transition fracture toughness $K_{JC(med)}$. It was considered that the CID as well as the local fracture stress σ_f^* may be a main control factor determining the fracture toughness characteristics in case of the applicability of the fracture stress model in the transition temperature region.

Acknowledgements

This work has been financially supported by the Korean Ministry of Science of Technology through the Reactor Pressure Boundary Materials Project.

References

[1] J. Malkin, A.S. Tetelman, Eng. Frac. Mech. 3 (1971) 131.
[2] R.O. Ritchie, B. Francis, W.L. Server, Metall. Trans. A 7A (1976) 831.
[3] R.O. Ritchie, W.L. Server, R.A. Wullaert, Metall. Trans. A 9A (1978) 331.
[4] D.A Curry, Met. Sci. 14 (1980) 319.
[5] J.H. Chen, G.Z. Wang, Z. Wang, L. Zhu, Y.Y. Gao, Metall. Trans. 22A (1992) 2287.
[6] J.H. Chen, G.Z. Wang, Metall. Trans. 23A (1992) 509.
[7] G.Z. Wang, J.H. Chen, Metall. Mater. Trans. A 27A (1996) 1909.
[8] D.M. Parks, J. Eng. Mater. Technol. 98 (1976) 30.
[9] S.P. Rawal, J. Gurland, Metall. Trans. A 8A (1977) 691.
[10] H.J. Rack, Mater. Sci. Eng. 24 (1976) 165.
[11] R. Hill, The Mathematical Theory of Plasticity, Clarendon, Oxford, 1950.
[12] J.R. Griffith, D.R. Owen, J. Mech. Phys. Solids 19 (1971) 419.
[13] G.Z. Wang, H.J. Wang, J.H. Chen, Fatigue Frac. Eng. Mater. Struct. 22 (1999) 849.
[14] P. Bowen, S.G. Druce, J.F. Knott, Acta Metall. 34 (1986) 1121.
[15] R.O. Richie, J.F. Knott, J.R. Rice, J. Mech. Phys. Solids 21 (1973) 395.
[16] K. Wallin, Eng. Frac. Mech. 19 (1984) 1085.
[17] K. Wallin, Eng. Frac. Mech. 22 (1985) 149.
[18] ASTM standard E 1921-97, 1997, Determination of Reference Temperature, T_0, for Ferritic Steels in the Transition Range, 1997.
[19] J.D. Landes, D.H. Shaffer, ASTM STP 700, American Society for Testing and Materials, 1980, p. 368.
[20] W. Weibull, J. Appl. Mech. 18 (1953) 293.
[21] J.H. Chen, L. Zhu, H. Ma, Acta. Metall. Mater. 38 (1990) 2527.
[22] R.M. McMeeking, J. Mech. Phys. Solids 25 (1977) 357.
[23] J.R. Rice, G.F. Rosengren, J. Mech. Phys. Solids 16 (1968) 1.
[24] J.W. Hutchinson, J. Mech. Phys. Solids 16 (1968) 13.
[25] J.R. Rice, M.A. Johnson, in: Inelastic Behavior of Solids, McGrawHill, New York, 1970, p. 641.
[26] D.A. Curry, J.F. Knott, Met. Sci. 10 (1976) 1.